An Infrared Investigation of the $(CO_2)_n^-$ Clusters: Core Ion Switching from Both the Ion and Solvent Perspectives

J.-W. Shin,[†] N. I. Hammer, and M. A. Johnson*

Sterling Chemistry Laboratory, Yale University, P. O. Box 208107, New Haven, Connecticut 06520

H. Schneider, A. Glöβ, and J. M. Weber

Institut für Physikalische Chemie, Universität Karlsruhe, Kaiserstr. 12, D-76128, Karlsruhe, Germany

Received: January 6, 2005; In Final Form: February 9, 2005

The $(CO_2)_n^-$ clusters are thought to accommodate the excess electron by forming a localized molecular anion, or "core ion", solvated by the remaining, largely neutral CO_2 molecules. Earlier studies interpreted discontinuities in the $(CO_2)_n^-$ photoelectron spectra to indicate that both the CO_2^- and $C_2O_4^-$ species were present in a size-dependent fashion. Here we use vibrational predissociation spectroscopy to unambiguously establish the molecular structures of the core ions in the $2 \leq n \leq 17$ size range. Spectra are reported in the 2300−3800 cm^{-1} region, which allows us to independently monitor the contribution of each ion through its characteristic overtone and combination bands. These signature bands are observed to be essentially intact in the larger clusters, establishing that the CO_2^- and $C_2O_4^-$ molecular ions are indeed the only electron accommodation modes at play. The size dependence of the core ion suggested in earlier analyses of the photoelectron spectra is largely confirmed, although both species are present over a range of clusters near the expected critical cluster sizes, as opposed to the prompt changes inferred earlier. Perturbations in the bands associated with the nominally neutral CO_2 "solvent" molecules are correlated with the changes in the molecular structure of the core ion. These observations are discussed in the context of a diabatic model for electron delocalization over the CO_2 dimer. In this picture, the driving force leading to the transient formation of the monomer ion is traced to the solvent asymmetry inherent in an incomplete coordination shell.

I. Introduction

When a cluster of atoms or molecules accommodates an excess electron to form the negatively charged species, several possibilities exist according to the availability of low-lying molecular orbitals. In water clusters, for example, there is very little penetration of excess electron density into the valence network, while metal clusters delocalize the charge over all of the nuclei. Most closed-shell molecular systems fall between these limits, and the excess charge is observed to localize on a smaller molecular structure embedded in an otherwise neutral cluster, where the remaining molecules play the role of a solvent. This is, of course, the cluster analogue of "polaron" formation in molecular crystals, a reconstruction that leads to thermally activated conduction of the negative charge carriers.[1] In clusters, the CO_2 system has attracted particular attention because it provides a paradigm for solvent-mediated deformation of the localized molecular framework that accommodates the excess charge. In previous studies,[2−4] the extent of charge-delocalization has been inferred from the cluster size-dependent patterns in the rather broad $(CO_2)_n^-$ photoelectron spectra. Here, we report vibrational predissociation spectra of the size-selected clusters, and show that they provide a much clearer picture of both the core ion structures and the intramolecular distortions suffered by the nominally neutral solvent molecules near the size-dependent ion core.

II. Review of the Core Ion Behavior in $(CO_2)_n^-$ Clusters: $C_2O_4^-$ vs CO_2^-

The CO_2^- monomer anion is itself interesting. Being isoelectronic with NO_2, the valence ion is bent (calculated $\theta = 134°$),[5] but this equilibrium configuration lies about 0.6 eV[6] above the ground state energy of the linear neutral parent and a free electron. The intersection between the anionic and neutral potential surfaces is such that the anion is locally stable with a substantial barrier to electron autodetachment, explaining the relatively long lifetime (100 μs) of this metastable species.[6−8] The binding energy of the excess electron is increased by solvation,[9−14] however, and the $(CO_2)_n^-$, $n \geq 2$, ions appear to be stable.

As with most negatively charged molecular clusters,[12,15−19] the dimer anions, A_2^-, are unique in that they are further stabilized by the charge-resonance interaction (i.e., mixing between the $A{\cdot}A^-$ and $A^-{\cdot}A$ charge-localized, diabatic states). When there is very little intramolecular geometry change upon electron attachment to form A^-, the two diabatic states remain degenerate under intramolecular distortion. In that case, introduction of the strong charge-transfer matrix element (typically 0.5−1.0 eV) generally results in a symmetrical dimer anion, in the sense that the excess charge is delocalized over the two molecular centers. The CO_2 system represents a more interesting class of systems, however, where the strong geometry change in the CO_2 moiety upon electron attachment leads to the displaced diabatic potential curves (i.e., arising from the zero-order $CO_2^-{\cdot}CO_2$ and $CO_2{\cdot}CO_2^-$ basis states) sketched in Figure 1. These curves are plotted along a reaction coordinate which

* To whom correspondence should be addressed.
[†] Present address: Imagene, 406 Biotechnology Incubating Center, Seoul National University, Seoul, South Korea 151-742.

10.1021/jp050092k CCC: $30.25
Published on Web 03/16/2005

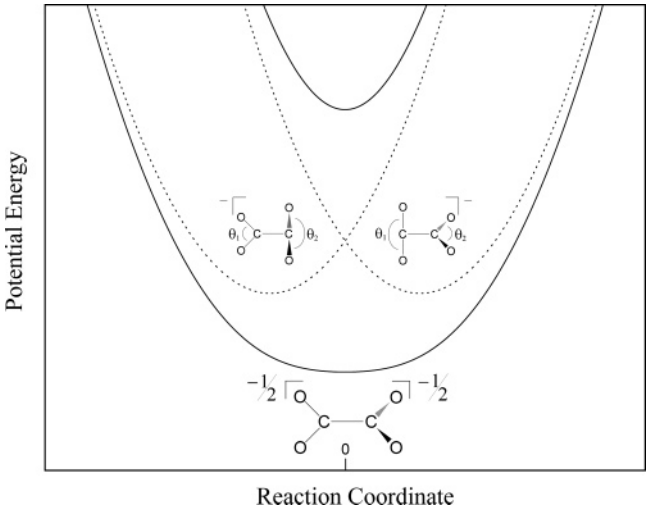

Figure 1. Charge-resonance mixing between the $CO_2 \cdot CO_2^-$ and $CO_2^- \cdot CO_2$ charge-localized diabatic states (dotted lines) yields a single-minimum potential (solid lines) for the $C_2O_4^-$ ion, where the reaction coordinate $\theta_R \cong \theta_1 - \theta_2$.

mediates interconversion of the two CO_2 constituents between the neutral and anionic forms. Since this conversion most strongly depends on the intramolecular bending angle, the coordinate has a large contribution from the collective motion described by $\theta_R = \theta_1 - \theta_2$. Note that the two curves are only degenerate at the point where both CO_2 component molecules are partially bent ($\theta_R = 0°$). When these diabatic states are split by introduction of the electron transfer matrix element to recover the actual surface (solid lines in Figure 1), the two states are strongly repelled only at the degeneracy point, with smaller displacements closer to the (double) minima of the diabatic curves. Depending on the size of the matrix element and the extent of the displacement between the diabats, the resulting dimer evolves from a double-minimum configuration, where the excess charge is localized on a monomeric (CO_2^-) species, to a single minimum potential where the charge is equally shared by the two molecules at the equilibrium geometry. The latter ($C_2O_4^-$) species can be regarded as the singly ionized analogue of the covalently bound oxalate anion, $C_2O_4^{2-}$. Of primary importance in the present study is the observation that we expect a relatively flat surface for motion along θ_R,[20] and displacement along this coordinate leads to large changes in the extent of delocalization of the excess charge. In other words, the system undergoes strong vibronic coupling along this coordinate, and is thus unusually polarizable.

Of course, we invoke the approximate diabatic picture to emphasize conceptual aspects of the binary complex electronic structure, and systems this small can be accurately treated using ab initio methods. Fleischman and Jordan[20] carried out such calculations on negatively charged CO_2 clusters in 1987 and predicted that the dimer anion would be symmetrical, with the $C_2O_4^-$ species adopting D_{2d} geometry, indeed reminiscent of the oxalate ion structure.

The theoretical expectation that the dimer anion is symmetrical, together with the fact that excursions away from equilibrium along the relatively flat potential surface lead to charge-localization, naturally raises the question of how this very polarizable species will respond when placed in a solvent. Fleischman and Jordan[20] considered this issue and suggested that the attachment of a CO_2 molecule should stabilize the system back toward the $CO_2 \cdot CO_2^-$ form, creating a situation where the core ion would likely depend on the size of the cluster. The underlying physics of this effect lies in following how the

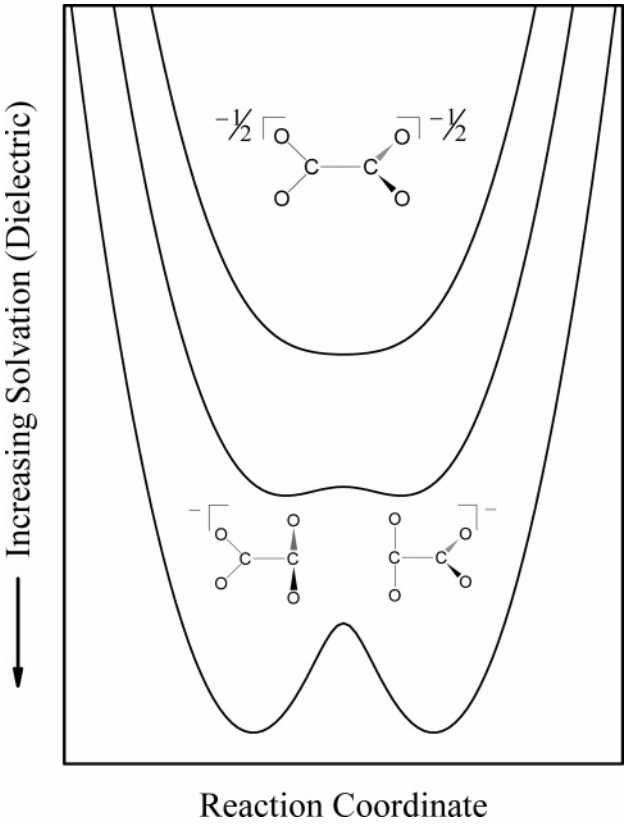

Figure 2. Schematic illustration of $C_2O_4^-$ solvation in a dielectric medium, indicating how a potential barrier can emerge and collapse the excess charge distribution onto a single CO_2 molecule.

shape of the potential curve in Figure 1 responds to solvation. Consider the extreme, limiting case where the dimer anion is placed in a dielectric continuum. According to the simple Born model for ion solvation[21] (i.e., $\Delta G_{solv} \propto 1/R_i$, where R_i is the radius of a spherical charge distribution), the charge-localized regions of the intrinsic dimer potential experience larger dielectric stabilization than the more delocalized symmetrical form. This differential solvation effect can thus cause the barrier to re-emerge in the dimer surface as indicated schematically in Figure 2, which describes a *solvent-induced* "switching" of the core ion from $C_2O_4^-$ to CO_2^-. Note that this effect can occur even in the case when an ion is placed in a homogeneous (spherical) dielectric.[22] Introduction of a molecular solvent thus raises the more interesting scenario where the "dielectric" can be added asymmetrically, and indeed the morphology of the system is likely to be size-dependent.

Several experimental groups[2−4,23] have explored the structures of the $(CO_2)_n^-$ ions using negative ion photoelectron spectroscopy. When the $CO_2^- \cdot CO_2$ and $C_2O_4^-$ species are close in energy, the vertical electron detachment energies (VDEs) differ by almost an electronvolt due to the larger geometry change of the neutral molecular framework in the $C_2O_4^-$ structure. Thus, Johnson and co-workers[2] interpreted the sharp breaks in the VDEs of the $(CO_2)_n^-$ clusters at $n = 2$ and 6 to reflect changes in the core ion, first from to CO_2^- to $C_2O_4^-$ at $n = 2$ and then reverting to the monomer core ion in the larger clusters ($6 \leq n \leq 13$). Nagata and co-workers[3] subsequently explored even larger sizes and, interestingly, observed *another* break in the VDE at $n = 14$, but in the opposite direction to that found around $n = 6$. This indicated that the dimer ion re-appears near the strong "magic numbers" at $n = 14$ and 16 in the ion distribution.[24] The $n = 6$ cluster is unique in that both ions appear to coexist in the sense that they could not be separated

using selective laser depopulation of the lower VDE, monomer anion-based form.[3] Very recently, Sanov and co-workers examined the $(CO_2)_n^-$ clusters ($n = 4-9$) using photoelectron imaging.[4] This added dimension allowed them to study the orbital nature of the two competing core ions. Interestingly, the photoelectron angular distributions of clusters turned out to be similar for all the clusters and are thus insensitive to the nature of the core ion. They attributed this similarity to the fact that the dimer core anion electronic structure can be largely expressed as a linear combination of two monomeric contributions.

Recent advances[25] in infrared spectroscopy now enable us to make much more definitive determinations of cluster ion structures, and here we report mid-infrared spectra of size-selected $(CO_2)_n^-$ clusters in the 2300−3800 cm^{-1} region. Clear spectral signatures of both core ions are observed, and we use this information to establish the relative contributions of the two classes of electron accommodation motif to the cluster ion ensemble created in an electron impact ion source.

III. Experimental Section

The $(CO_2)_n^-$ ($1 \le n \le 17$) clusters are produced by expansion of CO_2 vapor through a pulsed supersonic jet and are analyzed using tandem time-of-flight photofragmentation spectroscopy as described previously.[26] Briefly, bombardment of the expanding vapor by a counterpropagating 1-keV electron beam ionizes the CO_2 molecules, which produces slow secondary electrons that are efficiently attached to $(CO_2)_n$ clusters formed early in the expansion.

Vibrational predissociation spectra are obtained by excitation of the mass-selected clusters with a tunable infrared laser (Nd:YAG-pumped, KTP/KTA optical parametric oscillator/amplifier, LaserVision), which delivers an energy of about 5 mJ per pulse in a bandwidth of approximately 2 cm^{-1}. The mid-infrared beam is scanned over the range 2300−3800 cm^{-1}, and each spectrum represents the accumulation of many individual scans (depending on the parent intensity) as required to achieve comparable signal-to-noise ratios. Spectra are recorded using the instruments at Karlsruhe and Yale, where the larger spectral range of the Karslruhe infrared laser enables us to cover the region of the CO_2 ν_3 fundamental. The Karlsruhe instrument features mass selection using a pulsed mass gate,[27] and fragment ions due to metastable decay or collision-induced dissociation are discriminated against by employing a decelerating lens. This is advantageous because ions that decay in the source region reach the detector somewhat after the photodissociation products. For clusters above $n = 3$, photoexcitation results in evaporative loss of CO_2 molecules, with the number of CO_2 molecules ejected depending strongly on the parent size as reported earlier by Alexander et al.[24] In the cases of $(CO_2)_2^-$ and $(CO_2)_3^-$, photoinduced autodetachment of the excess electron competes with the fragmentation channel, and their spectra are obtained in the Yale instrument by collecting all photoelectrons generated in the excitation region using a constant extraction field of about 50 V/cm.

IV. Results and Discussion

A. Vibrational Characterization of the Core Ions. Figure 3 presents the predissociation spectra for $n = 3$ and 8, chosen to highlight the two distinct spectral signatures at play in the $(CO_2)_n^-$ clusters. Both spectra are dominated by a strong transition slightly to the red of 2349 cm^{-1}, which can be immediately assigned to the ν_3 fundamental of a neutral, nearly unperturbed CO_2 molecule. Two additional CO_2 bands appear

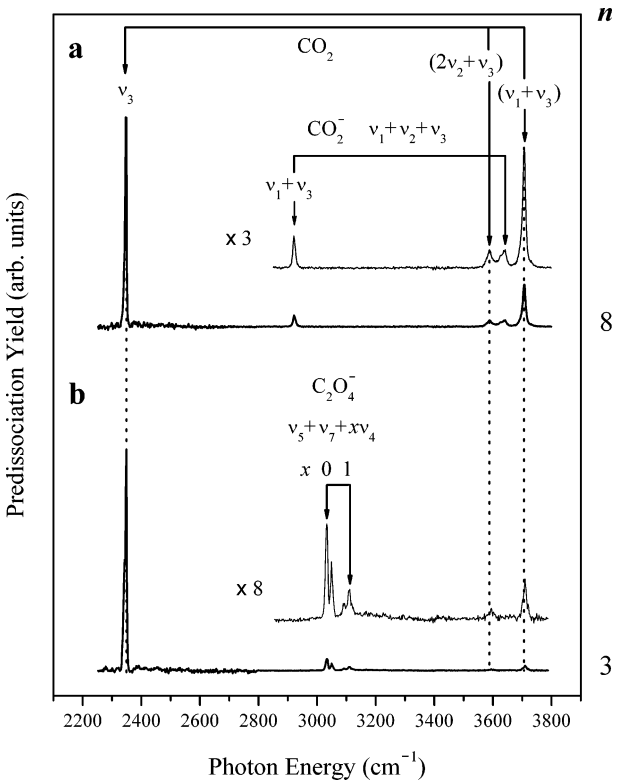

Figure 3. Predissociation spectra of $(CO_2)_n^-$ clusters, (a) $n = 8$ and (b) $n = 3$, showing spectral signatures of the monomer ($\nu_1 + \nu_3$ and $\nu_1 + \nu_2 + \nu_3$) and the dimer ($\nu_5 + \nu_7 + x\nu_4$) core ion combination bands, respectively. The $(2\nu_2 + \nu_3)/(\nu_1 + \nu_3)$ bands are built on the $2\nu_2/\nu_1$ Fermi resonant interaction in neutral CO_2.

at the upper end of the excitation energy range (e.g., at 3595 and 3710 cm^{-1} for $n = 3$) and are due to the (Fermi mixed) $2\nu_2 + \nu_3$ and $\nu_1 + \nu_3$ levels. This is an excited-state analogue of the well-known doubling observed for the ν_1 fundamental. These three bands signal the presence of neutral CO_2 species in the cluster, playing the anticipated role of solvent molecules in the cluster ions.

The smaller features lying between those arising from essentially neutral CO_2 are of primary interest here, and are observed to be highly dependent on cluster size. Two groups of such bands are evident, which typically appear exclusive of each other. These can be assigned to the CO_2^- and $C_2O_4^-$ anions with the aid of the rare gas matrix measurements reported by Thompson and Jacox.[28] They assigned the $\nu_1 + \nu_3$ transition of the CO_2^- monomer to a band at 2894.7 cm^{-1}, 27 cm^{-1} below the isolated 2921 cm^{-1} feature in Figure 3a. Because we anticipated that $n = 8$ would occur with a monomer core ion based on the photoelectron results, we assign the 2921 cm^{-1} feature to the $\nu_1 + \nu_3$ transition in a charge-localized CO_2^- moiety within the $(CO_2)_8^-$ cluster. The 27 cm^{-1} blue-shift relative to the rare gas (Ne) value is interesting, perhaps indicating that the monomer anion is slightly perturbed when embedded in the homogeneous cluster medium (i.e., the blue-shift could be a consequence of partial charge-transfer, for example, which would cause the intramolecular frequencies of the anion to increase toward those of neutral CO_2). The 2921 cm^{-1} ($\nu_1 + \nu_3$) feature is always accompanied by a second band about 710 cm^{-1} above it at 3636 cm^{-1}, which falls between the Fermi doublet associated with the neutral CO_2 molecules. This interloper lies very close to the expected location (3626.3 cm^{-1})[28] of the $\nu_1 + \nu_2 + \nu_3$ combination band of the monomer anion and is so assigned on this basis, as indicated in Figure 3a. Note that, even though the fundamental transitions of CO_2^-

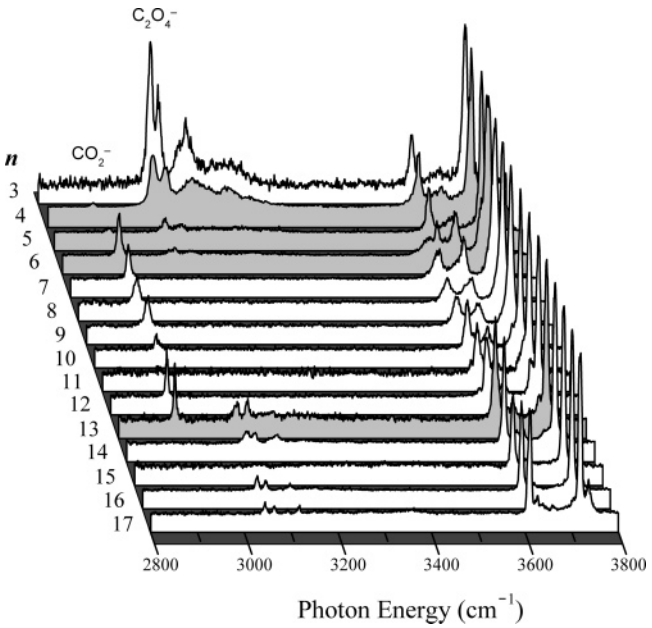

Figure 4. Survey of $(CO_2)_n^-$ spectra obtained from electron autodetachment ($n = 3$) and predissociation ($n \geq 4$). Spectra that are associated with a core ion switch are shaded gray. Labels denote bands assigned to CO_2^- and $C_2O_4^-$ (see Figure 3).

fall outside of the range of the lasers used in this work, these combination bands can be used to identify its presence within a cluster.

The second group of distinct bands displayed by the $(CO_2)_n^-$ clusters is indicated in Figure 3b and consists of a closely spaced set of peaks in the vicinity of 3100 cm^{-1}, well separated from the transitions associated with neutral CO_2 and the monomer anion, CO_2^-. These features appear in the spectra of the $3 \leq n \leq 6$ clusters, the size range where the photoelectron spectra[2-4] indicated the formation of a dimer core ion. Again, we turn to the matrix results to aid in the band assignments, where recent work on $C_2O_4^-$ in argon[29] identified the ν_5 symmetric (B_2) and ν_7 asymmetric (E) O−C−O stretching fundamentals to be at 1184.7 and 1856.7 cm^{-1}, respectively. Like the case of CO_2^-, all of the $C_2O_4^-$ fundamental transitions lie below the energy cutoff of the lasers used in this work, but a combination ($B_2 \times E = E$) of these two fundamentals yields an allowed transition at 3041.4 cm^{-1}, only 9 cm^{-1} above the most intense interloper between the neutral CO_2 based bands in Figure 3b. We therefore assign this band to the combination of ν_5 and ν_7. With the aid of our ab initio[30] (MP2/aug-cc-pVDZ) and the existing density functional theory[29] calculations, we identify the displacements corresponding to these modes to be principally the out-of-phase symmetric and asymmetric O−C−O stretching motions of the two CO_2 moieties in $C_2O_4^-$. Interestingly, this band is doubled with a shoulder split by 16 cm^{-1} on the high energy side, with a second feature displaced about 76 cm^{-1} above it. Comparison with the calculated[30] harmonic vibrations suggests that the latter band involves the relative torsion (ν_4) of the two CO_2 constituents in the $C_2O_4^-$ core.

B. Vibrational Spectra of the $(CO_2)_{3-17}^-$ Clusters: Size Dependence of the Core Ion. Figure 4 presents the evolution of the spectra with cluster size in the range $3 \leq n \leq 17$, isolating the signature regions of the CO_2^- and $C_2O_4^-$ ions. With the exception of $n = 3$, which is measured by electron photodetachment, these spectra are obtained by monitoring fragmentation into the loss-of-two CO_2 molecules channel. This selective detection scheme introduces a bias in the relative intensities as discussed below. Note that, as anticipated from the earlier photoelectron spectroscopy (PES) results,[3] the infrared spectra reveal that the core ion changes from the dimer to the monomer around $n = 6$ and then *back* to the dimer at $n = 14$, with the switchover regions indicated in gray. The vibrational spectra are more sensitive to the relative contributions from each core ion than PES because their IR transitions are mutually exclusive. Thus, it is now clear that both core ions contribute in the $n = 4-6$ clusters.

To extract the relative contributions from each isomer (differing by their core ions) to the ensemble of clusters, it is necessary to correct the raw data for both the changing fragmentation distributions and the relative absorption cross sections of the two core ions. For example, in the $n = 11$ and 15 clusters, which are just above very strong peaks in the parent mass spectrum, removal of a second CO_2 molecule from the stable $n = 10$ and 14 clusters is not observed, so that these spectra are severely compromised when selectively observed in the $n - 2$ fragmentation channel (in those cases, the $n - 1$ channel must therefore be employed in the population analysis). First, we correct the action spectra in Figure 4, which are taken by detecting the $n - 2$ fragment channel, $S_{n-2}(\nu)$, to recover the total fragment yield, $S(\nu)$, by independently measuring the fragmentation distribution at each wavelength. If $F_{n-2}(\nu)$ represents the fraction of fragments appearing in the $n - 2$ channel, $S(\nu)$ can be obtained from

$$S(\nu) = S_{n-2}(\nu)/F_{n-2}(\nu) \quad (1)$$

We can then use this net action spectrum $S_n(\nu)$ to estimate the relative cross sections of the two core ions. Here we adopt an approximate model where we assume that the intensities of the strongest bands (at ~3700 cm^{-1}) are proportional to the number of neutral CO_2 molecules. We can first check the validity of this hypothesis by considering cluster sizes that only display one type of core ion, so that the number of solvent molecules, m, contributing to the strong Fermi doublet is well defined. In that case, the integrated core ion absorption strength, I_{ion}, relative to that of a single CO_2 solvent molecule, I_{solv}, is related to the raw values in the spectra, $S(\nu_{ion})$ and $S(\nu_{solv})$, as

$$I_{ion}/I_{solv} = m \cdot S(\nu_{ion})/S(\nu_{solv}) \quad (2)$$

and should be constant over all clusters with the same core ion. This is indeed observed to be the case over the range $n = 7-12$ for the monomer core and $n = 14$, 16, and 17 for the dimer core. Since both of these relative absorption strengths involve internal calibration to the neutral CO_2 solvent absorption, we can then estimate that $I_{dimer}/I_{monomer} \sim 2.0$. With the relative cross sections in hand, it is straightforward to determine the relative contributions of the two core ions as a function of cluster size, which is presented in Figure 5.

C. Solvent Response to Core Ion Switching. The mechanism of the core switch is interesting, in that going from the dimer to the monomer core, for example, one of the CO_2 constituents in the dimer anion evolves into a neutral solvent molecule. Just at the transition, one might expect that the energies of the two forms are quite similar, and that one of the nominally neutral CO_2 molecules around a monomer core ion would be somewhat deformed according to the solvent configuration, effectively anticipating the delocalization event.

To explore the perturbations at play in the surrounding solvent, we focus on the bands arising from the neutral CO_2 molecules in Figure 6. Interestingly, the lower-energy band of the Fermi doublet undergoes a dramatic transformation during the core-ion switch from dimer to monomer around $n = 6$, first

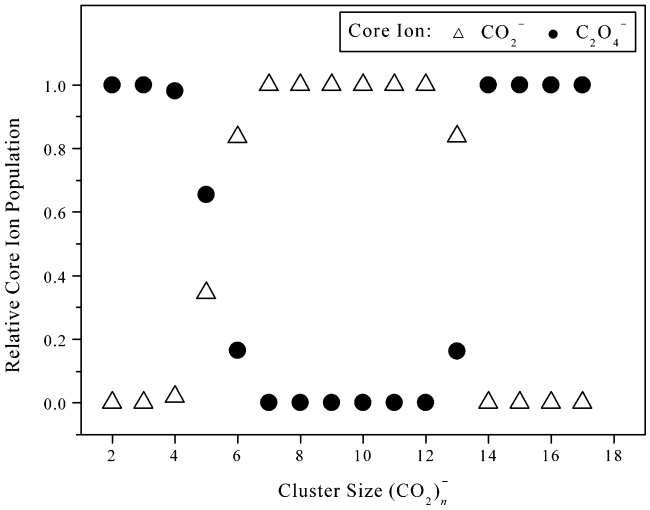

Figure 5. Relative abundance of monomer (triangles) and dimer (circles) core ions in the $(CO_2)_n^-$ clusters.

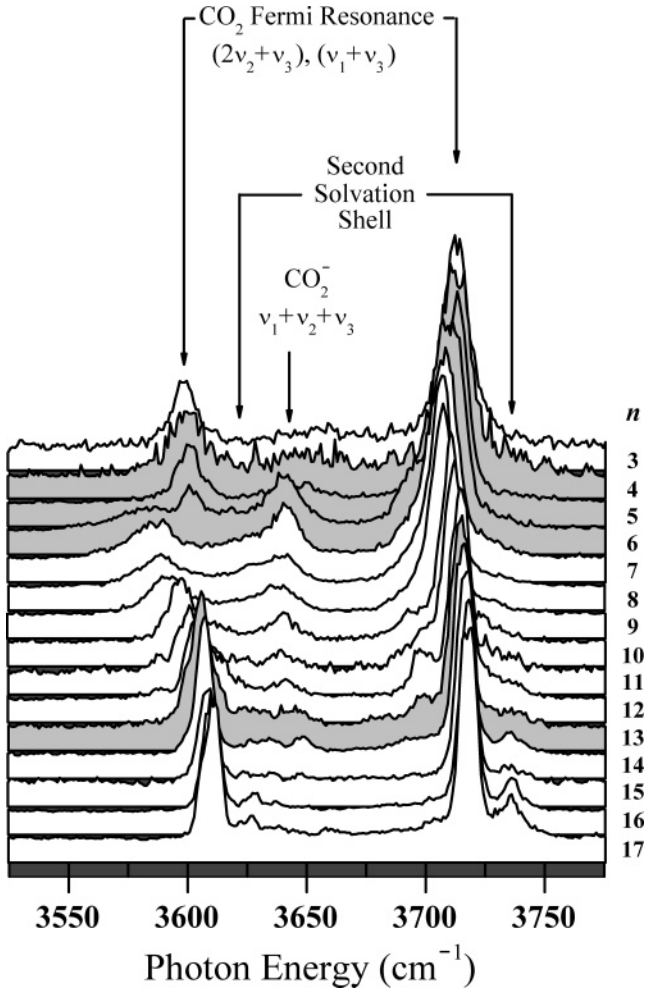

Figure 6. Expanded view of $(CO_2)_n^-$ spectra from Figure 3, highlighting the region of the CO_2 Fermi resonance. An abrupt red-shift in the lower-energy member of the diad, mostly derived from the $2\nu_2 + \nu_3$ level involving the intramolecular bend, is observed in the $n = 6$ spectrum. A band at higher energy also emerges above $n = 14$, signaling the beginning of a second solvation shell. Also visible in this region is the $\nu_1 + \nu_2 + \nu_3$ CO_2^- combination band, which is present in the monomer-core species $6 \leq n \leq 13$.

broadening and red-shifting, and then gradually returning to its original location and sharpening. Note that this feature involves the intramolecular bending motion (in the zero-order vibrational basis), and it is much more distorted than the stronger stretch-based transition at 3708 cm^{-1}. The latter (nominally $\nu_1 + \nu_3$) band develops a shoulder on the red side that gradually subsides with increasing cluster size until it reappears just before the second core switch at $n = 14$. The weaker deflection of the upper band mirrors the shift of the lower band, as would be expected if it were responding to the relieved Fermi mixing from a more distant perturber as opposed to directly interacting with the core ion.

The $n = 6$ spectrum displays the largest distortion, with the nominally $2\nu_2 + \nu_3$ transition appearing with a sharp peak on a broadened pedestal that extends about 30 cm^{-1} below the position of the band in isolated CO_2. This broadening is interesting in light of the hole-burning experiments reported by Nagata and co-workers,[3] which indicated that the two core ions interconvert on a ns time scale. Note that while this broadening is occurring in the solvent bands, the monomer core ion absorption at about 2920 cm^{-1} remains sharp (Figure 4).

A curious feature of the solvent-dependent $2\nu_2 + \nu_3$ band is that the entire envelope shifts down in energy and broadens after the first core switch. One might have expected, for example, that one CO_2 solvent molecule might be compromised by close association with the monomer core, while the remaining molecules would remain more or less intact. In such a case, the primary solvent band would have been maintained while a new band appeared at lower energy. Moreover, the observed band recovers its original location before the core switches back to the dimer at $n = 14$. One possibility is that the red-shift is a property of the excited bending vibrational states of neutral molecules near the monomer core ion. It is clear, for example, that this motion is the key coordinate that drives the charge transfer as depicted in Figure 1. When a solvent molecule is selectively excited along this coordinate, it seems likely that this bent configuration will experience enhanced electronic stabilization as the charge-transfer matrix element begins to mix the neutral solvent molecule with the ionic core. Thus, even in an inhomogeneous ensemble of solvent molecules, excited vibrational states of *each* molecule could be lowered. In this context, it seems likely that the observed broadening reflects the distribution of binding sites around the ion, and hence a range of electronic mixing interactions. In effect, the excited bending states retain a memory of the fact that the dimer core is energetically close in the size range above the core switch.

The solvent response to the second core switch near $n = 13$ is more subtle. The $n = 11$ spectrum is particularly interesting as it displays an unusually broad, low-energy tail on the $(2\nu_2 + \nu_3)$ bending overtone band, indicating that a subset of molecules are, in fact, becoming susceptible to charge transfer, ultimately leading to ground-state dimer core formation at $n = 14$. We also note, however, that $n = 11$ appears only one size above the more strongly bound $n = 10$ "magic number" species, and thus, some of the unique spectral characteristics of this size could arise from a variation in internal energy content for clusters near such discontinuities in monomer binding energy.

D. Origin of the Core Ion Switch: Solvent Asymmetry vs Intrinsic Delocalization. As mentioned in the introductory discussion, in the limit of solvation in a continuum dielectric medium with dielectric constant ϵ, a polarizable A_2^- core ion can be forced back to a charge-localized monomer ion as the dielectric constant is increased above a critical value.[22] With this in mind, the behavior of the homogeneous CO_2 cluster anions is curious since the first few solvent molecules indeed force charge localization, but then further increasing the number of solvent molecules leads to a reemergence of the dimer core

at $n = 14$. Thus, the CO_2 case is not driven by simple accumulation of dielectric medium, but is rather intimately linked to the molecular nature of the solvation.

The solvation morphologies in the size range where the $C_2O_4^-$ dimer is recovered have actually been studied extensively by the Lineberger and Neumark groups[31−34] in a series of "cage effect" photodissociation experiments. In particular, they interpreted the relatively prompt onset for geminate recombination of a photodissociated diatomic ion (such as I_2^-) upon addition of $n = 12-16$ CO_2 molecules to reflect the completion of a solvation shell around the ion. Indeed, the icosahedral cage-like structures associated with packing 12 spheres are well-known.[35] Moreover, the $n = 14$ cluster also appears as an unusually intense parent or "magic number" in the parent size distribution, as would be expected for such a closed shell structure.[13,36] The spectra associated with the nominally neutral CO_2 solvent molecules in Figure 6 also point to a shell closing around $n = 14$. Note that a distinct new band appears on the high energy sides of both the Fermi-split features, as would be expected when a binding site becomes available that is more remote from the ion core. The fact that the reemergence of the dimer core ion in the homogeneous $(CO_2)_n^-$ system coincides with the size where we expect the closure of the solvation shell around an ion roughly the size of I_2^- raises the strong possibility that the symmetry of the surrounding solvent is driving the structure of the core ion. This can be readily understood in the context of the diabatic picture outlined in Figure 1. As pointed out by Lineberger and co-workers,[31,32] the first few CO_2 molecules will likely bond to each other as well as the ion, naturally leading to an asymmetric "solvent cap" on one of the two monomeric components of the $C_2O_4^-$ dimer core ion. This causes preferential stabilitzation afforded to one of the monomer constituents within $C_2O_4^-$, breaking the degeneracy of the two parent diabatic states (Figure 1). When this differential solvation is sufficient to overcome the charge-resonance matrix element, the dimer collapses back to the monomer core. Interestingly, the critical size ($n = 6$) where the collapse occurs would correspond to a half-filled shell around the dimer anion. Note also that this was the size range where the caging experiments recovered a maximum in the spin−orbit relaxation of the excited halogen atom,[31,32] an effect traced to strong distortion in the I_2^- interatomic curves when placed in an asymmetrically solvated environment. As more solvent molecules are added, however, there will eventually be a sufficient number to surround the larger anionic core and eventually equally solvate both constituents of $C_2O_4^-$. In that case, the diabatic states would again become nearly degenerate, and the same charge-transfer matrix element can reestablish the delocalization over the dimer core ion configuration, as is observed. In essence, this competition between solvent-induced charge localization and the intrinsic propensity for delocalization through the charge-resonance interaction leads to a microscopic, molecular-level look at how the Marcus transition state for electron transfer[37] emerges as a consequence of the solvation mechanics.

V. Summary

The core ion switching behavior of the $(CO_2)_n^-$ clusters inferred from earlier photoelectron spectroscopy studies is largely confirmed using infrared spectroscopy to explicitly observe both the monomer and dimer core ions. The range of coexistence is determined to be three or four clusters rather than the prompt changes previously[2−4] reported. The bands arising from the bending motions of the neutral solvent molecules are observed to be strongly distorted near the core switches. We interpret this effect as due to the introduction of electronic mixing upon excitation of the intramolecular bending vibrations. That is, the nominally monomer ion-based clusters undergo charge delocalization in the vibrationally excited states of the nearby neutrals. The collapse to the monomer ion in the $n = 6-13$ range is traced to incomplete solvation in the asymmetrical $n = 6-11$ clusters. This can be understood in the context of underlying diabatic states, where one of the monomeric constituents of the dimer anion becomes preferentially stabilized in the asymmetric solvation regime, breaking the intrinsic propensity of this system to be charge-delocalized over two CO_2 molecules.

Acknowledgment. M.A.J. thanks the Department of Energy (Grant DR-FG02-00ER15066) for support of this work. J.M.W. gratefully acknowledges financial support from the Deutsche Forschungsgemeinschaft and Manfred M. Kappes for generous support and helpful discussion.

References and Notes

(1) Pope, M.; Swenberg, C. E. *Electronic Processes in Organic Crystals*; Oxford University Press: New York, 1982.
(2) DeLuca, M. J.; Niu, B.; Johnson, M. A. *J. Chem. Phys.* **1988**, *88*, 5857.
(3) Tsukuda, T.; Johnson, M. A.; Nagata, T. *Chem. Phys. Lett.* **1997**, *268*, 429.
(4) Mabbs, R.; Surber, E.; Velarde, L.; Sanov, A. *J. Chem. Phys.* **2004**, *120*, 5148.
(5) Almlöf, J.; Lund, A.; Thoumas, K.-Å. *Chem. Phys. Lett.* **1974**, *28*, 179.
(6) Compton, R. N.; Reinhardt, P. W.; Cooper, C. D. *J. Chem. Phys.* **1975**, *63*, 3821.
(7) Cooper, C. D.; Compton, R. N. *Chem. Phys. Lett.* **1972**, *14*, 29.
(8) Cooper, C. D.; Compton, R. N. *J. Chem. Phys.* **1973**, *59*, 3550.
(9) Schiedt, J.; Weinkauf, R. *Chem. Phys. Lett.* **1997**, *266*, 201.
(10) Lyapustina, S. A.; Xu, S.; Nilles, J. M.; Bowen, K. H., Jr. *J. Chem. Phys.* **2000**, *112*, 6643.
(11) Schiedt, J.; Knott, W. J.; Barbu, K. L.; Schlag, E. W.; Weinkauf, R. *J. Chem. Phys.* **2000**, *113*, 9470.
(12) Song, J. K.; Han, S. Y.; Chu, I.; Kim, J. H.; Kim, S. K.; Lyapustina, S. A.; Xu, S.; Nilles, M.; Bowen, K. H., Jr. *J. Chem. Phys.* **2002**, *116*, 4477.
(13) Hendricks, J. H.; Clercq, H. L. d.; Freidhoff, C. B.; Arnold, S. T.; Eaton, J. G.; Fancher, C.; Lyapustina, S. A.; Snodgrass, J. T.; Bowen, K. H. *J. Chem. Phys.* **2002**, *116*, 7926.
(14) Barbu, K. L.; Schiedt, J.; Weinkauf, R.; Schlag, E. W.; Nilles, J. M.; Xu, S.-J.; Thomas, O. C.; Bowen, K. H. *J. Chem. Phys.* **2002**, *116*, 9663.
(15) Bowen, K. H.; Liesegang, G. W.; Sanders, R. A.; Herschbach, D. R. *J. Phys. Chem.* **1983**, *87*, 557.
(16) Commita, P. B.; Brauman, J. I. *J. Am. Chem. Soc.* **1987**, *109*, 7591.
(17) Posey, L. A.; Johnson, M. A. *J. Chem. Phys.* **1988**, *88*, 5383.
(18) Tsukuda, T.; Hirose, T.; Nagata, T. *Int. J. Mass Spectrom. Ion Processes* **1997**, *171*, 273.
(19) Kelley, J. A.; Robertson, W. H.; Johnson, M. A. *Chem. Phys. Lett.* **2002**, *362*, 255.
(20) Fleischman, S. H.; Jordan, K. D. *J. Phys. Chem.* **1987**, *91*, 1300.
(21) Berry, R. S.; Rice, S. A.; Ross, J. *Physical Chemistry*, 2nd ed.; Oxford University Press: New York, 2000.
(22) McConnell, H. M. *J. Chem. Phys.* **1961**, *35*, 508.
(23) Bowen, K. H.; Eaton, J. G. Photodetachment Spectroscopy of Negative Cluster Ions. In *The Structure of Small Molecules and Ions*; Voger, R. N. a. Z., Ed.; Plenum: New York, 1988; Vol. 147, p 147.
(24) Alexander, M. L.; Johnson, M. A.; Levinger, N. E.; Lineberger, W. C. *Phys. Rev. Lett.* **1986**, *57*, 976.
(25) Johnson, M. S.; Kuwata, K. T.; Wong, C.-K.; Okumura, M. *Chem. Phys. Lett.* **1996**, *260*, 551.
(26) Johnson, M. A.; Lineberger, W. C. In *Techniques for the Study of Ion−Molecule Reactions*; Farrar, J. M., Saunders, W. H. J., Eds.; Wiley: New York, 1988; Vol. XX, p 591.
(27) Störmer, C. W.; Gilb, S.; Friedrich, J.; Schooss, D.; Kappes, M. M. *Rev. Sci. Instrum.* **1998**, *69*, 1661.
(28) Thompson, W. E.; Jacox, M. E. *J. Chem. Phys.* **1999**, *111*, 4487.
(29) Zhou, M.; Andrews, L. *J. Chem. Phys.* **1999**, *110*, 2414.

(30) Frisch, M. J.; Trucks, G. W.; Schlegel, H. B.; Scuseria, G. E.; Robb, M. A.; Cheeseman, J. R.; Zakrzewski, V. G.; Montgomery, J. A., Jr.; Stratmann, R. E.; Burant, J. C.; Dapprich, S.; Millam, J. M.; Daniels, A. D.; Kudin, K. N.; Strain, M. C.; Farkas, O.; Tomasi, J.; Barone, V.; Cossi, M.; Cammi, R.; Mennucci, B.; Pomelli, C.; Adamo, C.; Clifford, S.; Ochterski, J.; Petersson, G. A.; Ayala, P. Y.; Cui, Q.; Morokuma, K.; Malick, D. K.; Rabuck, A. D.; Raghavachari, K.; Foresman, J. B.; Cioslowski, J.; Ortiz, J. V.; Baboul, A. G.; Stefanov, B. B.; Liu, G.; Liashenko, A.; Piskorz, P.; Komaromi, I.; Gomperts, R.; Martin, R. L.; Fox, D. J.; Keith, T.; Al-Laham, M. A.; Peng, C. Y.; Nanayakkara, A.; Challacombe, M.; Gill, P. M. W.; Johnson, B.; Chen, W.; Wong, M. W.; Andres, J. L.; Gonzalez, C.; Head-Gordon, M.; Replogle, E. S.; Pople, J. A. *GAUSSIAN 98*; Gaussian, Inc.: Pittsburgh, 1998.

(31) Papanikolas, J. M.; Gord, J. R., Jr.; Levinger, N. E.; Ray, D.; Vorsa, V.; Lineberger, W. C. *J. Phys. Chem.* **19 91**, *95*, 8028.

(32) Sanov, A.; Lineberger, W. C. *Phys. Chem. Chem. Phys.* **2004**, *6*, 2018.

(33) Greenblatt, B. J.; Zanni, M. T.; Neumark, D. M. *J. Chem. Phys.* **2000**, *112*, 601.

(34) Gómez, H.; Taylor, T. R.; Neumark, D. M. *J. Chem. Phys.* **2002**, *116*, 6111.

(35) Corcelli, S. A.; Kelley, J. A.; Tully, J. C.; Johnson, M. A. *J. Phys. Chem. A* **2002**, *106*, 4872.

(36) Becker, I.; Cheshnovsky, O. *J. Chem. Phys.* **1999**, *110*, 6288.

(37) Marcus, R. A. *Can. J. Chem.* **1959**, *37*, 155.